Effects of trapped electrons on electromagnetic fields in an oblique shock wave

Mieko Toida[a] and Kenta Shikii
Department of Physics, Nagoya University, Nagoya 464-8602, Japan

(Received 15 July 2009; accepted 26 October 2009; published online 18 November 2009)

A magnetosonic shock wave propagating obliquely to an external magnetic field can trap electrons and accelerate them to ultrarelativistic energies. The effect of trapped electrons on electromagnetic fields in a shock wave is studied by theory and particle simulations. The expressions for field strengths are analytically obtained, including the number of trapped electrons n_t as a factor. It is shown that as n_t increases, the magnitude of F increases, where F is the integral of the parallel electric field, $E_\parallel=(\boldsymbol{E}\cdot\boldsymbol{B})/B$, along $\boldsymbol{B}$. Theoretical analysis also suggests that the increase in F causes the electrons to be trapped deeper and accelerated to higher kinetic energies. These theoretical predictions are verified with relativistic electromagnetic particle simulations. © *2009 American Institute of Physics*. [doi:10.1063/1.3264736]

I. INTRODUCTION

Theory and simulations[1] have found that prompt electron acceleration to ultrarelativistic energies with $\gamma > 100$, where γ is the Lorentz factor, can occur in a magnetosonic shock wave propagating obliquely to an external magnetic field with $|\Omega_e|/\omega_{pe} \gtrsim 1$, where $\Omega_e(<0)$ and ω_{pe} are the electron gyro- and plasma frequencies, respectively. This mechanism is expected to be important in the generation of energetic electrons in plasmas with strong magnetic fields such as solar magnetic tubes[2–4] and pulsars.[5] In an oblique shock wave, some electrons are reflected near the end of the main pulse of the wave and are trapped and energized in the main pulse region. [The shock wave approximates a train of solitons of decreasing amplitude[6,7] if the damping is small. (See, for instance, Fig. 3.5 in Ref. 7.) We call the first, leading pulse the main pulse.] Such electrons can get trapped when a negative dip of F is formed in the end of main pulse, where $F=-\int E_\parallel ds$ with $E_\parallel$ and ds being the electric field and infinitesimal length along the magnetic field, respectively. The trapped electrons oscillate in the main pulse region and the kinetic energies of electrons take maxima near the position of the peak of F. For this acceleration mechanism, a physical picture was given in Ref. 1 and a theory for the maximum energy was developed in Ref. 8 under the assumption that the wave is stationary. In these works, the effects of trapped electrons on wave evolution were not concerned, and the time variations in the electron maximum energy were not studied.

The simulations also demonstrated that once electrons are trapped, they cannot readily escape from the wave and are trapped deep in the main pulse region, which indicates that the number of trapped electrons increases continually with time.[8] In Ref. 9, the mechanism for the deep trapping was discussed. It was shown with theory and simulation that if $\partial F/\partial t > 0$ at particle positions, the parallel energies of the reflected electrons decrease, causing deep trapping. The reason for the increase in F is, however, unclear.

For the case of no trapped electrons, the theoretical expression for F has been recently given in Ref. 10, which shows that F can be large when the external magnetic field is strong. The study of $E_\parallel$ and F in nonlinear magnetosonic waves has also been extended to electron-positron-ion plasmas[11] because $E_\parallel$ plays a crucial role in the positron acceleration in oblique shock waves.[12]

Although the above many studies have been made on field strength and particle motion in an oblique shock wave, the feedback of the accelerated particles on the shock wave has never been investigated. Since the number of the trapped electrons increases with time, the effects of trapped electrons on wave evolution should be important. In this paper, we study this with theory and long-time simulations; we develop a theory for the field strength including the number of the trapped electrons as a factor, and compare it with the simulations. It is found that the trapped electrons strengthen $E_\parallel$ and F and that because of this, the magnitude of F increases with time. These results lead to the conclusion that the electrons are trapped deeper and accelerated to higher kinetic energies owing to the electromagnetic fields that they produce themselves.

In Sec. II, we analytically obtain expressions for electromagnetic fields in nonlinear magnetosonic waves in a plasma consisting of ions, electrons passing through the waves, and electrons trapped in the main pulse region. It is shown that the magnitude of F increases with the number of trapped electrons n_t. From this and previous simulation results,[1] we expect that F increases with time, in association with the increase in n_t. We then discuss how the time change in F affects the motions of trapped electrons. This analysis suggests that the electrons are trapped deeper and accelerated to higher kinetic energies as n_t increases. In Sec. III, the theoretical prediction is confirmed by a one-dimensional (one space coordinate and three velocity components) relativistic electromagnetic particle simulation. We show that both n_t and F continually increase with time. The relation between

[a]Electronic mail: toida@cc.nagoya-u.ac.jp.

the increment in F and that of n_t can be quantitatively explained by the theory. We also show that the maximum kinetic energy of the electrons grows, as predicted by the theory. In Sec. IV, we give a summary of our work.

II. THEORY FOR EFFECTS OF TRAPPED ELECTRONS ON *F*

We analytically study a nonlinear magnetosonic wave paying special attention to the effects of trapped electrons. It will be shown that the magnitude of F increases with the number of trapped electrons.

A. Basic equations

We consider a magnetosonic shock wave propagating in the x direction with a propagation speed $v_{\rm sh}$ in an external magnetic field in the (x,z) plane,

$$\boldsymbol{B}_{l0} = B_{l0}(\cos\theta, 0, \sin\theta), \tag{1}$$

where the subscript l refers to the quantities in the laboratory frame and the subscript 0 indicates the far upstream region. We suppose that the wave is stationary. Then, in the wave frame, the time derivatives of the quantities are zero, $\partial/\partial t = 0$, and Faraday's law gives the y and z components of the electric field as constants;

$$E_{wy} = E_{wy0} = -(v_{\rm sh}/c)B_{wz0} = -(v_{\rm sh}/c)\gamma_{\rm sh}B_{lz0}, \tag{2}$$

$$E_z = E_{wz0} = 0, \tag{3}$$

where the subscript w denotes the wave frame and $\gamma_{\rm sh} = (1-v_{\rm sh}^2/c^2)^{-1/2}$. For one-dimensional propagation with $\partial/\partial y = \partial/\partial z = 0$, the x component of the magnetic field is constant,

$$B_{wx} = B_{wx0} = B_{lx0}. \tag{4}$$

In the following, we analyze quantities in the wave frame, for which we omit the subscript w.

We suppose that the plasma consists of ions, electrons passing through the shock wave, and electrons trapped in the main pulse region. We can then write Gauss's and Ampere's laws in the wave frame as

$$\frac{dE_x}{dx} = 4\pi e(n_{\rm i} - n_e - n_{\rm t}), \tag{5}$$

$$\frac{dB_y}{dx} = \frac{4\pi}{c}(J_{\rm iz} + J_{\rm ez} + J_{\rm tz}), \tag{6}$$

$$\frac{dB_z}{dx} = -\frac{4\pi}{c}(J_{\rm iy} + J_{\rm ey} + J_{\rm ty}), \tag{7}$$

where the subscripts i, e, and t denote ions, passing electrons, and trapped electrons, respectively. We assume that the behavior of ions and passing electrons are described by the relativistic cold fluid model with zero time derivatives:

$$\frac{d}{dx}(n_j v_{jx}) = 0, \tag{8}$$

$$m_j v_{jx}\frac{d}{dx}(\gamma_j \boldsymbol{v}_j) = q_j \boldsymbol{E} + \frac{q_j}{c}\boldsymbol{v}_j \times \boldsymbol{B}, \tag{9}$$

where $j = $ i or e.

B. Physical picture

In this section, we present a physical picture for the effect of trapped electrons on F in an oblique shock wave. By virtue of Eqs. (2)–(4), we write the parallel electric field $E_\parallel$ in the wave frame as

$$E_\parallel = (E_x B_{x0} + E_{y0}B_y)/B, \tag{10}$$

from which F is given as

$$F = -\int ds E_\parallel = -\int_{x_0}^{x} dx E_\parallel B/B_{x0}, \tag{11}$$

where x_0 is a certain point in the far upstream region. This is also expressed, with the electric potential ϕ, as

$$F = \phi - \frac{E_{y0}}{B_{x0}}\int_{x_0}^{x} dx B_y. \tag{12}$$

The trapped electrons can generate B_y because they move along the magnetic field with parallel speed $v_\parallel \sim c$ in the main pulse region where $B_z \simeq B$. Assuming that the current of trapped electrons is given by $J_{\rm t} \sim (0,0,-en_{\rm t}c)$, we can estimate, from the z component of Ampere's law, the magnitude of B_y produced by the trapped electrons as

$$B_y^{(\rm t)} \sim -\frac{4\pi}{c}J_{\rm tz}\Delta_{\rm m} \sim 4\pi e n_{\rm t}\Delta_{\rm m}, \tag{13}$$

where $\Delta_{\rm m}$ is the width of the main pulse region and the index (t) indicates the quantities produced by the trapped electrons. From Eqs. (12) and (13), we obtain $F^{(\rm t)}$ as

$$F^{(\rm t)} \sim -4\pi\frac{E_{y0}}{B_{x0}}n_{\rm t}e\Delta_{\rm m}^2. \tag{14}$$

If $v_{\rm sh} \simeq c\cos\theta$ and $\Delta_{\rm m} \sim c/\omega_{\rm pe}$, Eq. (14) gives

$$eF^{(\rm t)} \sim (n_{\rm t}/n_{\rm e0})m_{\rm e}c^2. \tag{15}$$

This indicates that the magnitude of F increases with n_t.

C. Maximum values of B_z and ϕ

We now analyze, in more detail, the effects of trapped electrons on electromagnetic fields in a nonlinear magnetosonic wave. We first derive an expression for B_z including $n_{\rm t}$ and $\boldsymbol{J}_{\rm t}$. We multiply the x component of Eq. (9) by n_j and sum over ions and passing electrons to give

$$\sum_{j={\rm i,e}} m_j n_j v_{jx}\frac{d(\gamma_j v_{jx})}{dx} = \sum_{j={\rm i,e}} q_j n_j\left(E_x + \frac{v_{jy}}{c}B_z - \frac{v_{jz}}{c}B_y\right). \tag{16}$$

Combining Eqs. (5)–(7) and (16), we find that

$$\frac{d}{dx}\left(-\sum_{j=\mathrm{i,e}} m_j n_{j0} v_{\mathrm{sh}} \gamma_j v_{jx} + \frac{B_y^2+B_z^2-E_x^2}{8\pi}\right)$$
$$= eE_x n_{\mathrm{t}} - \frac{B_z}{c}J_{\mathrm{t}y} + \frac{B_y}{c}J_{\mathrm{t}z}, \quad (17)$$

where we have used the relation

$$n_j v_{jx} = -n_{j0} v_{\mathrm{sh}}, \quad (18)$$

which is obtained from Eq. (8). Equation (17) is integrated to give

$$\frac{B_y^2+B_z^2-B_{z0}^2-E_x^2}{8\pi} = \sum_{j=\mathrm{i,e}} m_j n_{j0} v_{\mathrm{sh}}(\gamma_{\mathrm{sh}} v_{\mathrm{sh}} + \gamma_j v_{jx}) + \int_{x_0}^{x} dx\left(eE_x n_{\mathrm{t}} - \frac{B_z}{c}J_{\mathrm{t}y} + \frac{B_y}{c}J_{\mathrm{t}z}\right). \quad (19)$$

We assume that B_z, the electric potential ϕ, and F have maximum values at the same point, $x=x_{\mathrm{m}}$, and that B_y and E_x are nearly zero at that point. This assumption is consistent with simulation results.[13] (For small-amplitude waves with no trapped electrons, this is analytically proved.[14]) Further, v_{jx} must be small in magnitude compared with the far upstream speed v_{sh} because the plasma density is high at $x=x_{\mathrm{m}}$. The maximum value of B_z, hence, satisfies the relation

$$\frac{B_{zm}^2-B_{z0}^2}{8\pi} \simeq m_{\mathrm{i}} n_0 \gamma_{\mathrm{sh}} v_{\mathrm{sh}}^2 + \int_{x_0}^{x_{\mathrm{m}}} dx\left(eE_x n_{\mathrm{t}} - \frac{B_z}{c}J_{\mathrm{t}y} + \frac{B_y}{c}J_{\mathrm{t}z}\right), \quad (20)$$

where $n_0 \simeq n_{\mathrm{e}0} \simeq n_{\mathrm{i}0}$. We suppose that in the right hand side of this equation, the second term, which is related to the trapped electrons, is much smaller than the first one. We then obtain B_{zm} as

$$B_{zm} \simeq B_{\mathrm{m}}^{(0)} + B_{\mathrm{m}}^{(\mathrm{t})}, \quad (21)$$

where the index $^{(0)}$ indicates the values for the case of no trapped electrons, and $B_{\mathrm{m}}^{(0)}$ and $B_{\mathrm{m}}^{(\mathrm{t})}$ are given as

$$B_{\mathrm{m}}^{(0)} \simeq \left(\frac{8\pi m_{\mathrm{i}} n_0 \gamma_{\mathrm{sh}} v_{\mathrm{sh}}^2}{B_{z0}^2} + 1\right)^{1/2} B_{z0}, \quad (22)$$

$$B_{\mathrm{m}}^{(\mathrm{t})} \simeq \frac{4\pi}{B_{\mathrm{m}}^{(0)}} \int_{x_0}^{x_{\mathrm{m}}} dx\left(eE_x n_{\mathrm{t}} - \frac{B_z}{c}J_{\mathrm{t}y} + \frac{B_y}{c}J_{\mathrm{t}z}\right). \quad (23)$$

Equation (22) is identical to Eq. (16) in Ref. 13, which was derived for the maximum B_z in a large-amplitude oblique shock wave, based on a cold two-fluid model. If $\gamma_{\mathrm{sh}} \sim 1$ and $v_{\mathrm{sh}} \gg v_{\mathrm{A}}$, $B_{\mathrm{m}}^{(0)}$ is approximated as

$$B_{\mathrm{m}}^{(0)}/B_0 \sim v_{\mathrm{sh}}/v_{\mathrm{A}}. \quad (24)$$

We next express E_x, ϕ, B_y, and $\boldsymbol{v}_{\mathrm{e}}$ in terms of B_z, n_{t}, and $\boldsymbol{J}_{\mathrm{t}}$. We suppose that $B_z \gg B_y$ and that the inertia of passing electrons is small in the momentum equation (9). Then, from the x, y, and z components of Eq. (9) for passing electrons, we have, respectively,

$$E_x = -v_{\mathrm{e}y} B_z / c, \quad (25)$$

$$v_{\mathrm{e}x} = cE_{y0}/B_z = -v_{\mathrm{sh}} B_{z0}/B_z, \quad (26)$$

$$B_y = (v_{\mathrm{e}y}/v_{\mathrm{e}x}) B_x. \quad (27)$$

Because ion currents can be neglected in Ampere's law [Eqs. (6) and (7)] (see the Appendix), $v_{\mathrm{e}y}$ and $v_{\mathrm{e}z}$ are written as

$$v_{\mathrm{e}y} = -\frac{c v_{\mathrm{e}x}}{4\pi e n_{\mathrm{e}0} v_{\mathrm{sh}}}\left(\frac{dB_z}{dx} + \frac{4\pi}{c}J_{\mathrm{t}y}\right), \quad (28)$$

$$v_{\mathrm{e}z} = \frac{c v_{\mathrm{e}x}}{4\pi e n_{\mathrm{e}0} v_{\mathrm{sh}}}\left(\frac{dB_y}{dx} - \frac{4\pi}{c}J_{\mathrm{t}z}\right). \quad (29)$$

Combining Eqs. (25), (26), and (28), we find

$$E_x = \frac{-B_{z0}}{4\pi e n_{\mathrm{e}0}}\left(\frac{dB_z}{dx} + \frac{4\pi}{c}J_{\mathrm{t}y}\right). \quad (30)$$

Integrating this from $x=x_0$ to $x=x_{\mathrm{m}}$, we obtain the maximum value of the electric potential as

$$e\phi_{\mathrm{m}} = e\phi_{\mathrm{m}}^{(0)} + e\phi_{\mathrm{m}}^{(\mathrm{t})}, \quad (31)$$

where $\phi_{\mathrm{m}}^{(0)}$ and $\phi_{\mathrm{m}}^{(\mathrm{t})}$ are given as

$$e\phi_{\mathrm{m}}^{(0)} = \frac{B_{z0}}{4\pi n_{\mathrm{e}0}}(B_{\mathrm{m}}^{(0)} - B_{z0}), \quad (32)$$

$$e\phi_{\mathrm{m}}^{(\mathrm{t})} = \frac{B_{z0}}{4\pi n_{\mathrm{e}0}}\left(B_{\mathrm{m}}^{(\mathrm{t})} + \frac{4\pi}{c}\int_{x_0}^{x_{\mathrm{m}}} dx J_{\mathrm{t}y}\right). \quad (33)$$

From Eqs. (27) and (28), we have

$$B_y = \frac{v_{\mathrm{e}y}}{v_{\mathrm{e}x}} B_x = -\frac{cB_x}{4\pi e n_{\mathrm{e}0} v_{\mathrm{sh}}}\left(\frac{dB_z}{dx} + \frac{4\pi}{c}J_{\mathrm{t}y}\right). \quad (34)$$

It follows that the assumption $|B_y| \ll B_z$ is valid when

$$\frac{\Delta}{(c/\omega_{\mathrm{pe}})} \frac{B_{zM}^2}{B_x(B_{zm}-B_{z0})} \gg \left(\frac{m_{\mathrm{i}}}{m_{\mathrm{e}}}\right)^{1/2}, \quad (35)$$

where Δ is the characteristic width of the shock transition region. Substituting Eq. (34) in Eq. (29) gives

$$v_{\mathrm{e}z} \simeq \frac{c^2 B_x B_{z0}}{(4\pi e n_{\mathrm{e}0})^2 v_{\mathrm{sh}} B_z}\left(\frac{d^2 B_z}{dx^2} + \frac{4\pi}{c}\frac{dJ_{\mathrm{t}y}}{dx}\right) + \frac{B_{z0}}{e n_0 B_z}J_{\mathrm{t}z}. \quad (36)$$

D. Estimate of *F*

We derive expressions for $E_\parallel$ and F. The above Eqs. (30) and (34) yield $E_\parallel = (E_x B_x + E_y B_y)/B = 0$. This indicates that to obtain $E_\parallel$ and F, we have to consider the electron inertial terms that were neglected in the above subsection. Including those terms in Eq. (9), we obtain E_x, $v_{\mathrm{e}x}$, and B_y as

$$E_x = -\frac{v_{\mathrm{e}y}}{c}B_z + \frac{v_{\mathrm{e}z}}{c}B_y - \frac{m_{\mathrm{e}} v_{\mathrm{e}x}}{e}\frac{d(\gamma_{\mathrm{e}} v_{\mathrm{e}x})}{dx}, \quad (37)$$

$$v_{\mathrm{e}x} = \frac{c}{B_z}E_{y0} + v_{\mathrm{e}y}\frac{B_x}{B_z} + \frac{m_{\mathrm{e}} c}{e B_z} v_{\mathrm{e}x}\frac{d(\gamma_{\mathrm{e}} v_{\mathrm{e}y})}{dx}, \quad (38)$$

$$B_y = \frac{v_{ey}}{v_{ex}} B_x - \frac{m_e c}{e} \frac{d(\gamma_e v_{ez})}{dx}. \quad (39)$$

Substituting Eq. (39) in Eq. (37) gives

$$E_x = -\frac{v_{ey} B_z}{c v_{ex}} \left(v_{ex} - v_{ey} \frac{B_x}{B_z} \right) - \frac{m_e}{e} \left(v_{ex} \frac{d(\gamma_e v_{ex})}{dx} + v_{ez} \frac{d(\gamma_e v_{ez})}{dx} \right), \quad (40)$$

which can be rewritten, by virtue of Eqs. (28) and (38), as

$$E_x = -\frac{B_{z0}}{4\pi e n_{e0}} \left(\frac{dB_z}{dx} + \frac{4\pi}{c} J_{ty} \right) - \frac{m_e c^2}{e} \frac{d\gamma_e}{dx}. \quad (41)$$

Also, substituting Eq. (28) in Eq. (39), we have

$$B_y = -\frac{c B_x}{4\pi e n_{e0} v_{sh}} \left(\frac{dB_z}{dx} + \frac{4\pi}{c} J_{ty} \right) - \frac{m_e c}{e} \frac{d(\gamma_e v_{ez})}{dx}. \quad (42)$$

From Eqs. (10), (41), and (42), we find that

$$E_\parallel = -\frac{m_e c^2}{e} \frac{B_{x0}}{B} \frac{d\gamma_e}{dx} - \frac{m_e c}{e} \frac{E_{y0}}{B} \gamma_e \frac{dv_{ez}}{dx}. \quad (43)$$

Integrating this, we obtain F as

$$eF = m_e(\gamma_e - \gamma_{sh}) c^2 + \frac{E_{y0}}{B_{x0}} m_e \gamma_e c v_{ez}. \quad (44)$$

If $\gamma_e, \gamma_{sh} \sim 1$, Eq. (44) can be estimated as

$$eF \sim \frac{E_{y0}}{B_{x0}} m_e c v_{ez}. \quad (45)$$

Substituting Eq. (36) in Eq. (45) and using the approximation $B_{z0} \sim B_0$, we get

$$F = F^{(0)} + F^{(t)}, \quad (46)$$

where $F^{(0)}$ and $F^{(t)}$ are

$$eF^{(0)} \sim -m_i v_A^2 \frac{c^2}{\omega_{pe}^2} \frac{1}{B_z} \left(\frac{d^2 B_z}{dx^2} \right), \quad (47)$$

$$eF^{(t)} \sim \frac{4\pi}{c} \frac{dJ_{ty}}{dx} - m_e v_{sh} \frac{B_0^2}{B_z B_{x0}} \frac{J_{tz}}{n_{e0} e}. \quad (48)$$

We note that Eq. (47) is valid for both small and large-amplitude waves if Eq. (35) is satisfied. When the wave amplitude is quite small, $\delta \equiv (B_z - B_{z0})/B_{z0} \ll 1$, $F^{(0)}$ is reduced to Eq. (30) in Ref. 10, which was obtained using a modified perturbation scheme assuming that δ is in the range $(m_e/m_i) \ll \delta \ll 1$.[15] For large-amplitude waves, we can use the approximations $d^2 B_z/dx^2 \sim -(B_m - B_{z0})/(c/\omega_{pe})^2$ and $dJ_{ty}/dx \sim J_{ty}/(c/\omega_{pe})$, because the width of the shock transition region is of the order of c/ω_{pe}, as shown by simulations in the next section. We then find that the maximum F is expressed as

$$F_m = F_m^{(0)} + F_m^{(t)}, \quad (49)$$

where $F_m^{(0)}$ and $F_m^{(t)}$ are given as

$$eF_m^{(0)} \sim m_i v_A^2 (B_m^{(0)} - B_0)/B_m, \quad (50)$$

$$eF_m^{(t)} \sim m_i v_A^2 \frac{B_m^{(t)}}{B_m} - m_e c \frac{|\Omega_e|}{\omega_{pe}} \frac{B_0}{B_m} \frac{J_{ty}}{n_{e0} e} - m_e v_{sh} \frac{B_0^2}{B_m B_{x0}} \frac{J_{tz}}{n_{e0} e}. \quad (51)$$

If the wave amplitude is $\delta \sim 1$, $F_m^{(0)}$ can be estimated as $eF_m^{(0)} \sim \delta m_i v_A^2$. This is identical to Eq. (35) with $T_e = 0$ in Ref. 10, which is a phenomenological relation that fits well with the simulation results for the case of $\boldsymbol{J}_t \simeq 0$.

E. Effects of trapped electrons on fields

We have obtained the expressions B_z, ϕ, and F that include n_t and $\boldsymbol{J}_t$. In this subsection, by estimating these quantities, we show that the effects of trapped electrons on B_z and ϕ are negligibly small, while that on F is significant.

We first consider the motion of a trapped electron in a perfectly stationary, one-dimensional wave. For this particle, we can derive an energy conservation form[1]

$$m_e c^2 \gamma - eF + c p_z \frac{E_{y0}}{B_{x0}} = \varepsilon, \quad (52)$$

where γ is the Lorentz factor and the energy ε is constant. This can be written as

$$\gamma h = \varepsilon + eF \quad (53)$$

where h is defined as

$$h = m_e c^2 \left(1 + \frac{v_z E_{y0}}{c B_{x0}} \right) = m_e c^2 \left(1 - \frac{v_z v_{sh} B_{z0}}{c^2 B_{x0}} \right), \quad (54)$$

which indicates that h is positive if B_{z0}/B_{x0} is of order unity.[1] If F is in the region $0 < F < F_m$, particles with energies in the region $-eF_m < \varepsilon < 0$ are trapped.

Using the drift approximation, we write the velocity of a trapped electron as

$$\boldsymbol{v} = v_\parallel \frac{\boldsymbol{B}}{B} + c \frac{\boldsymbol{E} \times \boldsymbol{B}}{B^2} \quad (55)$$

where we have neglected ∇B-drift (and other unimportant drifts) and the gyration velocity. The gyration velocity is unimportant in this trapping and acceleration mechanism.[1] Because $B_z \simeq B$ in the shock region, v_x is written as

$$v_x = v_\parallel \frac{B_x}{B} + c \frac{E_{y0}}{B}. \quad (56)$$

Since in the main pulse region, $|v_\parallel|$ can be of the order of c and can be much greater than $\boldsymbol{E} \times \boldsymbol{B}$ drift, we can approximate γ as

$$\gamma \simeq \sqrt{1 + p_\parallel^2/(m_e c)^2}, \quad (57)$$

where $p_\parallel$ is the parallel momentum ($p_\parallel = m_e \gamma v_\parallel$). Substituting Eq. (57) in Eq. (52), we have

$$m_e c^2 \sqrt{1 + p_\parallel^2/(m_e c)^2} - eF + c p_\parallel \frac{E_{y0}}{B_{x0}} = \varepsilon. \quad (58)$$

Differentiating Eq. (58) with t yields

$$\frac{dp_{\parallel}}{dt} = e\frac{B_x}{B}\frac{\partial F}{\partial x}, \tag{59}$$

where we have used Eq. (56).

We next derive the density and current of trapped electrons, n_t and $\boldsymbol{J}_{\rm t}$. We suppose that the distribution function of trapped electrons is written as $f_{\rm t}(x,p_{\parallel})$. The density of trapped electrons is then given as

$$n_{\rm t}(x) = \int_{-\infty}^{\infty} dp_{\parallel} f_{\rm t}(x,p_{\parallel}). \tag{60}$$

The distribution function $f_{\rm t}(x,p_{\parallel})$ is assumed to satisfy the stationary Vlasov equation

$$v_x\frac{\partial f_{\rm t}}{\partial x} + \frac{dp_{\parallel}}{dt}\frac{\partial f_{\rm t}}{\partial p_{\parallel}} = 0. \tag{61}$$

Since the coordinate x and momentum $p_{\parallel}$ are related through Eq. (58), $f_{\rm t}$ can be expressed as a function of ε; $f_{\rm t}(\varepsilon)$ satisfies Eq. (61) because of Eqs. (56) and (59). From Eqs. (56) and (58), we get the relation between $dp_{\parallel}$ and $d\varepsilon$ as

$$dp_{\parallel} = \frac{B_x}{B}\frac{d\varepsilon}{v_x}. \tag{62}$$

Since the particles with ε in the range $0<\varepsilon<eF_{\rm m}$ are trapped in the main pulse region, we can write Eq. (60) with the aid of Eq. (62) as

$$n_{\rm t} = \int_{-eF_M}^{0} d\varepsilon f_{\rm t}(\varepsilon)\frac{B_x}{B}\left(\frac{1}{v_{x+}} + \frac{1}{v_{x-}}\right), \tag{63}$$

where the velocities v_{x+} and v_{x-} are v_x of trapped particles going forward and backward, respectively. Because $|v_{\parallel}|\sim c$ in the main pulse region, $v_{x\pm}$ are estimated as

$$v_{x\pm} \sim \pm c\frac{B_x}{B}\left(1 \pm \frac{E_{y0}}{B_{x0}}\right). \tag{64}$$

When $v_{\rm sh}\simeq c\cos\theta$, they become

$$v_{x\pm} \sim \pm(c\cos\theta \mp v_{\rm sh})B_0/B, \tag{65}$$

namely, $v_{x+}\sim 0$ and $v_{x-}\sim -2c\cos\theta B_0/B$. Since the term proportional to $1/v_{x+}$ is dominant in the right hand side of Eq. (63), we obtain $n_{\rm t}$ as

$$n_{\rm t} \sim \frac{\cos\theta}{(c\cos\theta - v_{\rm sh})}\int_{-eF_M}^{0} d\varepsilon f_{\rm t}(\varepsilon). \tag{66}$$

The current of trapped electrons is written as

$$\boldsymbol{J}_{\rm t} \simeq -e\int_{-\infty}^{\infty} dp_{\parallel} f_{\rm t}(x,p_{\parallel})\left(c\frac{\boldsymbol{B}}{B} + c\frac{\boldsymbol{E}\times\boldsymbol{B}}{B^2}\right), \tag{67}$$

which, by virtue of Eqs. (62) and (66), gives

$$\boldsymbol{J}_{\rm t} \simeq -en_{\rm t}c\left(\frac{\boldsymbol{B}}{B} + \frac{\boldsymbol{E}\times\boldsymbol{B}}{B^2}\right). \tag{68}$$

Since $B_z\sim B$ in the shock region, we have

$$J_{\rm tz} \sim -en_{\rm t}c, \tag{69}$$

$$J_{\rm ty} \sim -en_{\rm t}c(B_y - E_x)/B. \tag{70}$$

If $v_{\rm sh}\simeq c\cos\theta$ and $B_{\rm m}>B_0$, $|J_{\rm tz}|$ is much greater than $|J_{\rm ty}|$. This can be explained as follows. Substituting Eqs. (30) and (34) in Eq. (70), we can write J_{ty} as

$$J_{\rm ty} \sim en_{\rm t}(c\cos\theta - v_{\rm sh})\frac{v_A}{v_{\rm sh}}\frac{c}{\omega_{\rm pe}}\left(\frac{m_{\rm i}}{m_{\rm e}}\right)^{1/2}\frac{1}{B}\frac{dB_z}{dx}. \tag{71}$$

Using Eq. (24) and the estimation that $dB_z/dx\sim(B_{\rm m}-B_0)/\Delta$, we have the ratio between $|J_{\rm ty}|$ and $|J_{\rm tz}|$ as

$$\frac{|J_{\rm ty}|}{|J_{\rm tz}|} \sim \frac{(c\cos\theta - v_{\rm sh})}{c}\frac{B_0(B_{\rm m}-B_0)}{B_{\rm m}^2\Delta}\frac{c}{\omega_{\rm pe}}\left(\frac{m_{\rm i}}{m_{\rm e}}\right)^{1/2}, \tag{72}$$

which is much smaller than unity if Eq. (35) is satisfied.

Using Eqs. (69)–(71), we now estimate $B_{\rm m}^{(\rm t)}$, $\phi_{\rm m}^{(\rm t)}$, and $F_{\rm m}^{(\rm t)}$. Substituting Eqs. (69) and (70) in Eq. (23) gives

$$B_{\rm m}^{(\rm t)} \sim 0. \tag{73}$$

The effect on trapped electrons on $B_{\rm m}$ is thus negligible. From Eqs. (33), (72), and (73), we obtain $\phi_{\rm m}$(t) as

$$e\phi_{\rm m}^{(\rm t)} \sim m_{\rm e}c(c\cos\theta - v_{\rm sh})\frac{|\Omega_e|}{\omega_{\rm pe}}\frac{n_{\rm t}}{n_{\rm e0}}\frac{B_0(B_{\rm m}-B_0)}{B_{\rm m}^2}. \tag{74}$$

We can therefore expect that if $v_{\rm sh}\simeq c\cos\theta$, $\phi_{\rm m}^{(t)}$ would be quite small. The magnitude of $F_{\rm m}^{(\rm t)}$ can be estimated from Eq. (51) as

$$eF_{\rm m}^{(\rm t)} \sim m_{\rm e}v_{\rm sh}c\frac{n_{\rm t}}{n_{\rm e0}}\frac{B_0^2}{B_{x0}B_m} \sim m_{\rm e}c^2\frac{n_{\rm t}}{n_{\rm e0}}\frac{B_0}{B_{\rm m}}, \tag{75}$$

which is identical to Eq. (15) when $B_{\rm m}/B_0$ is of order unity. We thus find that the effect of trapped electrons on $F_{\rm m}$ is significant and that the magnitude of $F_{\rm m}$ increases with the number of trapped electrons n_t.

F. Electron motion in nonstationary *F*

Particle simulation demonstrates that once electrons are trapped in the main pulse region, they cannot readily escape from it and the number of trapped electrons n_t continually increases with time.[1,9] Since Eq. (75) suggests that the magnitude of F increases with n_t, we here suppose that F gradually grows with time in association with the increase in $n_{\rm t}$ and then discuss how the time change in F affects the motion of trapped electrons.

We assume that F at time t is written as

$$F(x,t) = F^{(0)}(x)[1 + \alpha n_{\rm t}(t)], \tag{76}$$

where $n_{\rm t}(t)$ is the number density of trapped electrons at time t, $F^{(0)}(x)$ is given by Eq. (47), and α is of constant order,

$$\alpha \sim \frac{1}{n_{\rm t}}\frac{F_{\rm m}^{(\rm t)}}{F_{\rm m}^{(0)}} \sim \frac{1}{n_{\rm e0}}\frac{\omega_{\rm pe}^2}{|\Omega_{\rm e}|^2}\frac{B_0}{B_{\rm m}^{(0)}}. \tag{77}$$

For nonstationary F, we can derive an energy equation of electrons as[9]

$$\frac{d\varepsilon}{dt} = -e\frac{\partial F}{\partial t} \simeq -e\alpha F^{(0)}(x)\frac{dn_t}{dt}. \qquad (78)$$

This indicates that if $dn_t/dt > 0$, the energy ϵ decreases, which gives rise to deep trapping of electrons; just as a particle oscillating in a potential well with damping. We therefore find that the electrons become more deeply trapped owing to the electromagnetic fields that they produce themselves.

The increase in F enhances the acceleration of trapped electrons. The theoretical expression for the Lorentz factor γ of trapped particles was given in Ref. 8 where the wave field was assumed to be stationary. We here extend the theory to the case for the nonstationary F. We may write γ of the particle at time t and position x as

$$\gamma(x,t) = \frac{\varepsilon(t) + eF(x,t)}{m_e c(c + v_\parallel E_{y0}/B_{x0})}. \qquad (79)$$

Since $\varepsilon(t) \lesssim 0$ for trapped particles and $F(x,t) \le F_m(t)$, where $F_m(t)[\equiv F(x_m,t)]$ is the maximum F at time t, the upper limit of γ is given as

$$\gamma_{\lim}(t) = \frac{eF_m(t)\cos\theta}{m_e c(c\cos\theta - v_{sh})}, \qquad (80)$$

where we have used $v_\parallel \simeq c$. The upper limit of γ of the trapped particles is proportional to $F_m(t)$. From Eqs. (50) and (77), the value of $\gamma_{\lim}$ can be estimated as

$$\gamma_{\lim} \sim \frac{\Omega_e^2}{\omega_{pe}^2}\left(1 + \frac{n_t}{n_{e0}}\frac{\omega_{pe}^2}{|\Omega_e|^2}\frac{B_0}{B_m^{(0)}}\right)\left(1 - \frac{v_{sh}}{c\cos\theta}\right)^{-1}, \qquad (81)$$

which indicates that if v_{sh} is close to $c\cos\theta$, γ can be much greater than unity.

We now consider the time variation in γ of a trapped particle. We suppose that the particle gets trapped at time t_0 and its γ takes maximum values γ_m at times $t_1, t_2, \cdots$, at which the particle is near the position $x = x_m$ with $v_\parallel \simeq c$. The value of γ_m can then be estimated from Eq. (79) as

$$\gamma_m(t_n) = \frac{[\varepsilon(t_n) + eF_m(t_n)]\cos\theta}{m_e c(c\cos\theta - v_{sh})}, \qquad (82)$$

where n is an integer. To obtain $\varepsilon(t_n)$, we integrate Eq. (78) from t_0 to t_n, giving

$$\varepsilon(t_n) - \varepsilon(t_0) = -e\int_{t_0}^{t_n} dt\,\alpha\frac{dn_t}{dt}F_0(x)$$
$$\sim -e\alpha\langle F^{(0)}\rangle[n_t(t_n) - n_t(t_0)], \qquad (83)$$

where $\langle F^{(0)}\rangle$ is the average of $F^{(0)}$ over the main pulse region. Using the approximation $\langle F^{(0)}\rangle \sim F_m^{(0)}/2$, we can write $\gamma_m(t_n)$ as

$$\gamma_m(t_n) \sim \frac{e[F_m(t_n) + F_m(t_0) + \varepsilon(t_0)]\cos\theta}{2m_e c(c\cos\theta - v_{sh})}. \qquad (84)$$

From this, we can expect that if F_m increases, γ_m also increases.

III. SIMULATIONS

In this section, using a one-dimensional (one space coordinate and three velocities), relativistic, electromagnetic particle code with full ion and electron dynamics, we simulate an oblique shock wave and confirm that the number of trapped particles n_t, the magnitude of F, and the maximum energies of electrons grow with time. For the method of particle simulations and excitation of shock waves, see Refs. 1 and 16.

As in the theory in Sec. II, the shock wave propagates in the x direction in an external magnetic field $\boldsymbol{B}_0 = B_0(\cos\theta, 0, \sin\theta)$. The propagation angle is set to be $\theta = 45°$. The total system length is $L = 16\,384\Delta_g$, where Δ_g is the grid spacing. The system length is four times longer than that in the previous works.[1,8,9] The number of ions and electrons are $N_i = N_e \simeq 1.0 \times 10^7$, which are 50 times greater than those in the previous simulations. By using these values, we can reduce noise[20] and can clearly show how the trapped electrons affect the wave evolution for a long-time. The mass ratio is $m_i/m_e = 100$. The ratio of gyrofrequency and plasma frequency of electrons is $|\Omega_e|/\omega_{pe} = 3.0$ in the upstream region. The light speed is $c/(\omega_{pe}\Delta_g) = 4.0$ and the electron and ion thermal velocities in the upstream region are $v_{Te}/(\omega_{pe}\Delta_g) = 0.5$ and $v_{Ti}/(\omega_{pe}\Delta_g) = 0.05$, respectively. The Alfven speed is then $v_A/(\omega_{pe}\Delta_g) = 1.2$. From Eq. (81), which indicates that the value of γ is independent of those of m_i/m_e, c/v_A, and v_{Te}/c, we can expect that in the case of those values being close to real ones, the strong acceleration would occur if v_{sh} is close to $c\cos\theta$. We here present the simulation results for the shock wave with v_{sh} being 96% of the $c\cos\theta$.

Figure 1 shows electron phase space plots (x, γ) and magnetic field profiles of a shock wave with a propagation speed $v_{sh} = 2.64$ at times $\omega_{pe}t = 480$, 740, and 1300. In the top panel ($\omega_{pe}t = 480$), we find some electrons are trapped and accelerated to ultrarelativistic energies with $\gamma > 50$ in the main pulse region, $478 < x/(c/\omega_{pe}) < 485$. At $\omega_{pe}t = 740$, more particles are trapped and the maximum γ exceeds 100. At $\omega_{pe}t = 1300$, the number of trapped electrons increases and the maximum energy reaches $\gamma \simeq 200$.

Figure 2 displays the profiles of F (dashed line) and B_z (solid line). F and B take their maximum values at almost the same positions. The peak value of F at $\omega_{pe}t = 480$, at which the number of trapped particles is small, is observed to be $eF/(m_e c^2) \sim 9$. This is in good agreement with the theoretical value, $eF/(m_e c^2) \sim 7$, which was obtained from Eq. (50) using $n_t \simeq 0$ and the observed value of B_m. The peak value of F at $\omega_{pe}t = 1300$ is greater than those at $\omega_{pe}t = 480$ and 740.

Figure 3 shows the time variations in the maximum values of B_z, ϕ, and F. In the bottom panel, the time variation in the number density of trapped electrons is plotted. (Here, n_t is approximated as N_t/Δ_m, where Δ_m is the width of the main pulse region and N_t is the number of energetic electrons with $\gamma > 10$ in the main pulse region; the trapped electrons can have such high energies, while the transmitted ones have energies of, at most, $\gamma = 10$.) As predicted by the theory [Eqs. (73) and (74)], B_z and ϕ are almost constant although n_t increases with time. The magnitude of F, however, increases

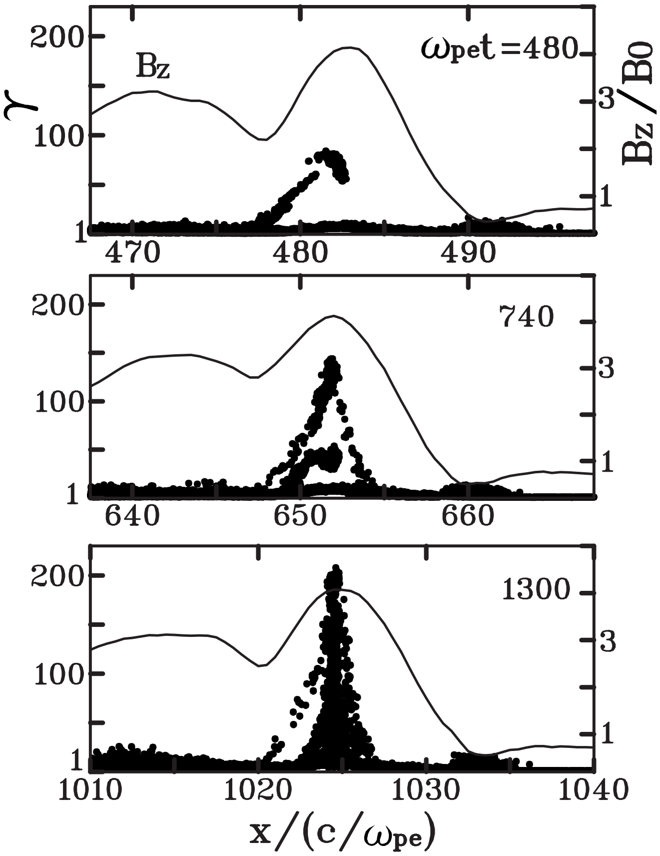

FIG. 1. Phase space plots (x,γ) of electrons and magnetic field profiles at $\omega_{pe}t=480$, 740, and 1300.

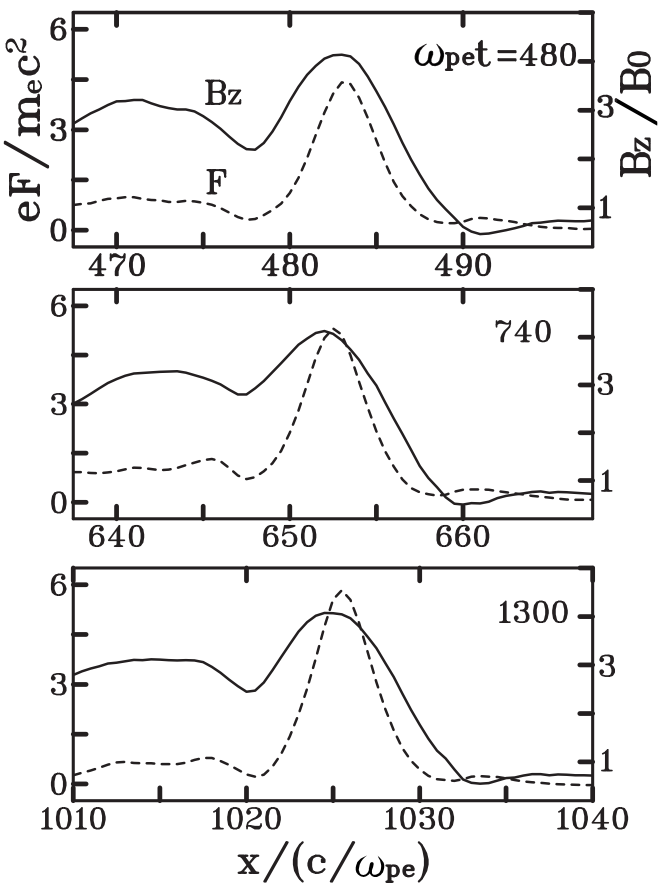

FIG. 2. Profiles of B_z (solid lines) and F (dashed lines) at $\omega_{pe}t=480$, 740, and 1300.

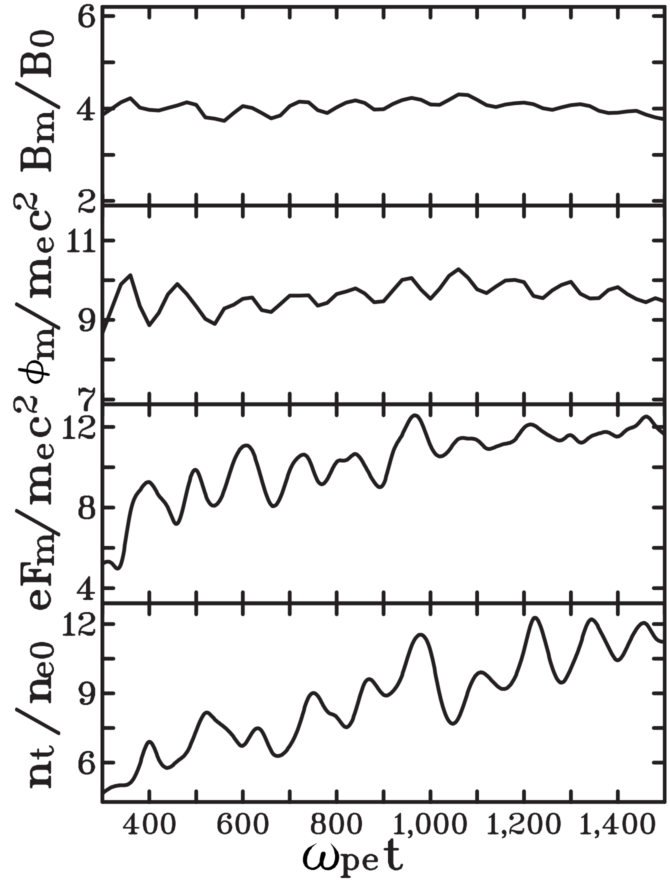

FIG. 3. Time variations in B_m, ϕ_m, F_m, and the number density of trapped electrons, n_t. The values of F_m and n_t increase with time, while B_m and ϕ_m are almost constant.

with an increase in n_t. The increment in F_m from $\omega_{pe}t=400$ to 1300 is observed to be $e\Delta F_m/(m_e c^2) \simeq 3$, which is the same order of magnitude as the theoretical value based on Eq. (75). Substituting the observed value of the increment in n_t for this period, $n_t/n_{e0} \simeq 5$, in Eq. (75) gives $e\Delta F_m/(m_e c^2) \simeq 2$. It is thus clearly shown that F_m grows owing to the effect of the trapped electrons. {The oscillations of B_m, ϕ_m, F_m, and n_t with the period $\omega_{pe}t \simeq 70[\simeq (2\pi/3) \times (\omega_{pe}/\Omega_i)]$ are due to the ion reflection at the shock front.[17–19]}

We now present results showing that the increase in F can enhance the electron acceleration. Figure 4 shows time variations in the observed value of the maximum γ of the electrons (black line). The maximum γ increases on average with time, due to the increase in F_m. The gray line in Fig. 4 indicates the theory [Eq. (80)] for the upper limit of γ, where we have substituted the observed value of F_m in Eq. (80) and have averaged over the time period of the amplitude oscillation due to the ion reflection, $\omega_{pe}t=70$. The profiles of γ_m and γ_{lim} are similar and their values are in the same order of magnitude. We can therefore confirm that the increase in γ_m is caused by that of F_m.

The trajectory of a trapped electron is depicted in Fig. 5, where the time variations in $x-x_m$, γ, $v_\parallel$, and $v_\perp$ are shown. The electron encounters the shock wave at $\omega_{pe}t \simeq 300$. At $\omega_{pe}t \simeq 400$, it is reflected at the end of the main pulse and

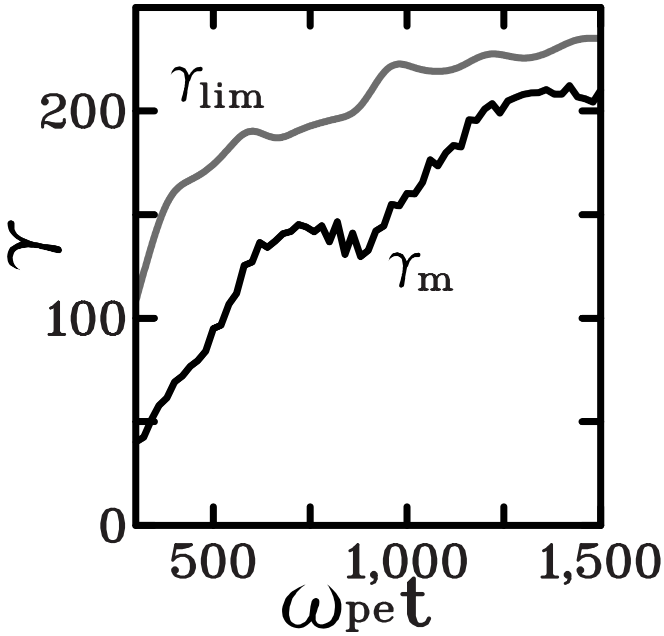

FIG. 4. Time variations in the maximum value of γ of electrons. The simulation result (black line) is similar to the theory (gray line) for the upper limit of γ given by Eq. (80).

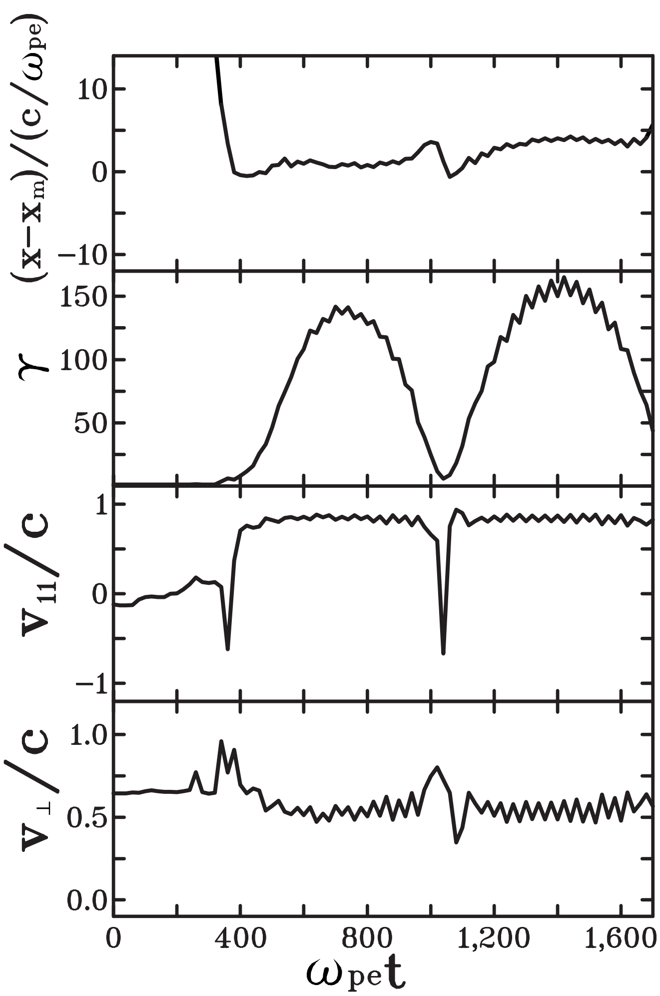

FIG. 5. Time variations in $x-x_m$, γ, $v_\parallel$, and $v_\perp$ of a trapped electron.

gets trapped in the main pulse region. It moves forward relative to the shock wave with $v_\parallel \simeq c$. Its kinetic energy becomes maximum near the center of the main pulse, $x \simeq x_m$, at $\omega_{pe}t=700$. The electron is then reflected backward in the shock transition region at $\omega_{pe}t \simeq 1000$. It soon reaches the end of the main pulse and is again reflected forward. Its kinetic energy becomes maximum at $\omega_{pe}t \simeq 1400$. Note that the second peak of γ at $\omega_{pe}t \simeq 1400$ is higher than the first one at $\omega_{pe}t \simeq 700$. This is due to the increase in F. The difference between the two maximum γ's, $\Delta\gamma_m \simeq 16$, can be explained by Eq. (82); substituting the observed value of the increase in F_m from $\omega_{pe}t=700$ to $\omega_{pe}t=1400$ in Eq. (82), we have $\Delta\gamma_m \simeq 20$.

IV. SUMMARY

A magnetosonic shock wave propagating obliquely to an external magnetic field can trap electrons and accelerate them to ultrarelativistic energies. Once the electrons are trapped, they cannot readily escape from the wave and the number of trapped electrons continually increases with time. The parallel electric field and its integral F along the magnetic field play crucial roles in this trapping and acceleration mechanism.

In order to investigate the effect of the trapped electrons on electromagnetic fields in a shock wave, we derive expressions for field strengths in an oblique shock wave in a plasma consisting of ions, electrons passing through the waves, and electrons trapped in the main pulse region. We find that the magnitude of F increases with the number of trapped electrons n_t. We suggest that owing to the increase in F, the electrons are trapped deeper and are accelerated to higher kinetic energies.

Particle simulations demonstrate that both F and n_t increase with time and that associated with this increase, the kinetic energies of the trapped electrons grow. The theoretical predictions have thus been verified by the simulations.

We note that the theory and simulations are both one-dimensional in the present and previous studies. As future work, it would be important to study multidimensional effects on the trapping and acceleration mechanisms.

APPENDIX: ION VELOCITIES

We here present the condition for ion currents to be neglected in Ampere's law. We multiply the y component of Eq. (9) by n_j and sum over ions and passing electrons to give

$$\sum_{j=\mathrm{i,e}} m_j n_j v_{jx} \frac{d(\gamma_j v_{jy})}{dx} = \sum_{j=\mathrm{i,e}} q_j n_j \left(E_y + \frac{v_{jz}}{c} B_x - \frac{v_{jx}}{c} B_z \right). \tag{A1}$$

Assuming that the electron inertial term can be neglected in the left-hand side in Eq. (A1), we obtain v_{iy} as

$$v_{iy} \simeq -\frac{B_{x0}}{4\pi n_0 m_i \gamma_i v_{sh}} B_y - \frac{eE_{y0}}{n_0 m_i \gamma_i v_{sh}} n_t + \frac{1}{m_i n_0 \gamma_i v_{sh} c} \int dx (J_{tz} B_{x0} - J_{tx} B_z), \tag{A2}$$

where we have used the x component of Ampere's law

$$e(n_i v_{ix} - n_e v_{ex}) + J_{tx} = 0. \tag{A3}$$

In the right hand side of Eq. (A2), the first term is dominant. From the z component of Ampere's law [Eq. (7)], we can write v_{ey} as

$$v_{ey} \simeq v_{iy} - \frac{c v_{ex}}{4\pi e n_0 v_{sh}} \frac{dB_z}{dx} + \frac{1}{n_e e} J_{ty}, \tag{A4}$$

where we have used the approximation $n_e \simeq n_i$. Substituting Eq. (34) in Eq. (A2), we can estimate the ratio between the first and second terms in the right hand side of Eq. (A4) as

$$v_{iy} \Bigg/ \left(\frac{c v_{ex}}{4\pi e n_0 v_{sh}} \frac{dB_z}{dx} \right) \sim \frac{B_{x0}^2}{B_{zm} B_0}. \tag{A5}$$

This is much smaller than unity. We can therefore neglect the ion current in the z component of Ampere's law.

As for v_{iz}, we obtain from the z component of Eq. (9),

$$v_{iz} \simeq -\frac{B_{x0}}{4\pi n_0 m_i \gamma_i v_{sh}} (B_z - B_{z0}) + \frac{1}{m_i n_0 \gamma_i v_{sh} c} \int dx (J_{tx} B_y - J_{ty} B_x). \tag{A6}$$

The y component of Ampere's law can be rewritten as

$$v_{ez} \simeq v_{iz} + \frac{c v_{ex}}{4\pi e n_0 v_{sh}} \frac{dB_y}{dx} + \frac{1}{n_e e} J_{tz}. \tag{A7}$$

With the aid of Eq. (34), we can estimate the ratio between the first and second term in the right hand side of Eq. (A7) as

$$v_{iz} \Bigg/ \left(\frac{c v_{ex}}{4\pi e n_0 v_{sh}} \frac{dB_y}{dx} \right) \sim \left(\frac{m_e}{m_i} \right) \frac{\Delta^2 \omega_{pe}^2}{c^2} \frac{B_{zm}}{B_0}. \tag{A8}$$

Assuming that this ratio is smaller than unity, we neglect the effect of v_{iz} in the y component of Ampere's law.

[1] N. Bessho and Y. Ohsawa, Phys. Plasmas **6**, 3076 (1999).
[2] D. J. Forrest and E. K. Chupp, Nature (London) **305**, 291 (1983).
[3] H. Nakajima, T. Kosugi, K. Kai, and S. Enome, Nature (London) **305**, 292 (1983).
[4] S. R. Kane, E. L. Chupp, D. J. Forrest, G. H. Share, and E. Rieger, Astrophys. J. Lett. **300**, L95 (1986).
[5] F. A. Aharonian, A. G. Akhperjanian, J. A. Barrio, K. Bernlöhr, H. Bojahr, I. Calle, J. L. Contreras, J. Cortina, S. Denninghoff, V. Fonseca, J. C. Gonzalez, N. Götting, G. Heinzelmann, M. Hemberger, G. Hermann, A. Heusler, W. Hofmann, D. Horns, A. Ibarra, R. Kankanyan, M. Kestel, J. Kettler, C. Köhler, A. Kohnle, A. Konopelko, H. Kornmeyer, D. Kranich, H. Krawczynski, H. Lampeitl, A. Lindner, E. Lorenz, F. Lucarelli, N. Magnussen, O. Mang, H. Meyer, R. Mirzoyan, A. Moralejo, L. Padilla, M. Panter, R. Plaga, A. Plyasheshnikov, J. Prahl, G. Pühlhofer, G. Rauterberg, A. Röhring, V. Sahakian, M. Samorski, M. Schilling, D. Schmele, F. Schröder, W. Stamm, M. Tluczykont, H. J. Völk, B. Wiebel-Sooth, C. Wiedner, M. Willmer, and W. Wittek, Astrophys. J. **539**, 317 (2000).
[6] R. Z. Sagdeev, in *Reviews of Plasma Physics*, edited by M. A. Leontovich (Consultants Bureau, New York, 1966), Vol. 4, p. 23.
[7] D. A. Tidman and N. A. Krall, *Shock Waves in Collisionless Plasmas* (Wiley-Interscience, New York, 1971).
[8] N. Bessho and Y. Ohsawa, Phys. Plasmas **9**, 979 (2002).
[9] A. Zindo, Y. Ohsawa, N. Bessho, and R. Sydora, Phys. Plasmas **12**, 052321 (2005).
[10] S. Takahashi and Y. Ohsawa, Phys. Plasmas **14**, 112305 (2007).
[11] S. Takahashi, M. Sato, and Y. Ohsawa, Phys. Plasmas **15**, 082309 (2008).
[12] H. Hasegawa, S. Usami, and Y. Ohsawa, Phys. Plasmas **10**, 3455 (2003); H. Hasegawa, K. Kato, and Y. Ohsawa, *ibid.* **12**, 082306 (2005).
[13] S. Miyahara, T. Kawashima, and Y. Ohsawa, Phys. Plasmas **10**, 98 (2003).
[14] T. Kakutani, H. Ono, T. Taniuti, and C. C. Wei, J. Phys. Soc. Jpn. **24**, 1159 (1968).
[15] M. Toida and Y. Ohsawa, J. Phys. Soc. Jpn. **63**, 573 (1994).
[16] P. C. Liewer, A. T. Lin, J. M. Dawson, and M. Z. Caponi, Phys. Fluids **24**, 1364 (1981).
[17] D. Biskamp and H. Welter, Nucl. Fusion **12**, 663 (1972).
[18] R. L. Tokar, S. P. Gary, and K. B. Quest, Phys. Fluids **30**, 2569 (1987).
[19] T. Kawashima, S. Miyahara, and Y. Ohsawa, J. Phys. Soc. Jpn. **72**, 1664 (2003).
[20] A. B. Langdon and C. K. Birdsall, Phys. Fluids **13**, 2115 (1970).